

# Compact $E$ parallel $B$ type end-loss ion mass-resolving energy analyzer

Yousuke Nakashima, Minoru Yokoyama,<sup>a)</sup> Yoshio Imai,<sup>b)</sup> Kiyoshi Yatsu, and Syoichi Miyoshi

Plasma Research Center, University of Tsukuba, Tsukuba, Ibaraki 305, Japan

(Received 7 February 1989; accepted for publication 21 April 1989)

A compact  $E$  parallel  $B$  ( $E \parallel B$ ) type end-loss ion mass-resolving energy analyzer was fabricated and tested. In the analyzer, a small-angle deflection magnet and a preaccelerator/decelerator of end-loss ions are adopted in order to reduce the size and to expand an energy range with a sufficient energy resolution. Orbit calculations in the  $E \parallel B$  fields including the influence of fringe fields were made by a Monte Carlo code in which the effects of finite radius and angle of the incident ions are taken into consideration. Preliminary measurements on the GAMMA 10 tandem mirror were successfully performed and it was confirmed that the analyzer has capabilities for the spectrometer of end-loss ions.

Ions escaping from the mirror-confined plasma along the magnetic field line have significant information, such as plasma potential and ion temperature. The absolute measurement of their fluxes makes it possible to study the properties of axial particle confinement. A conventional multi-gridded end-loss analyzer (ELA)<sup>1</sup> has been used for the measurement of ions escaping from the end region of tandem mirrors. The ELA has high sensitivity and can measure the energy distribution of end-loss ions by scanning the retarding voltage applied on the ELA's grid. However, during discharges with strong plugging, the ELA is occasionally affected by high-energy electrons which make it difficult to detect a small amount of end-loss ions due to the limitation of electron-retarding voltage.

Recently, an  $E$  parallel  $B$  ( $E \parallel B$ ) type end-loss ion spectrometer (ELIS) was constructed and applied to the TMX-U tandem mirror in Lawrence Livermore National Laboratory.<sup>2,3</sup> This type of analyzer, which has been developed for a mass-resolving neutral particle energy analyzer,<sup>4,5</sup> effectively separates the electron and ions. The ELIS is also capable of making a detailed analysis of the energy distribution with fast time resolution. However, the ELIS usually occupies a large space because it uses a large  $180^\circ$  bending magnet and a massive magnetic shield. Therefore, it is difficult to set several ELIS's in an array for the simultaneous measurement of the spatial profile.

In this letter, we describe a compact  $E \parallel B$  type end-loss ion mass-resolving energy analyzer in which a bending magnet with a small deflection angle is used. After the calibration experiments,<sup>6</sup> the analyzer was installed at the end cell of the GAMMA 10 tandem mirror.<sup>7,8</sup> Preliminary measurements were made in order to evaluate the capabilities of the analyzer.

The fabricated analyzer has the following features. To reduce the size of the analyzer, a  $45^\circ$  deflection magnet is used in contrast with the conventional  $180^\circ$  magnet of the ELIS. An accelerator/decelerator is provided at the entrance of the analyzer. The preacceleration method has been applied to the charge-exchange neutral particle analyzer in JAERI.<sup>9</sup> In the measurement of lower energy ions ( $< 500$

eV), the accelerator is used for the analysis with a higher  $E \parallel B$  field in order to obtain a wide energy coverage. The decelerator is used for the measurement at a higher energy range ( $> 1000$  eV) in order to analyze ions with higher energy resolution by reducing the  $E \parallel B$  field. The above mechanisms enable us to analyze the end-loss ions with the energy range 100–2000 eV in a sufficient energy resolution. The analyzer also has a capacity for the mass resolution between hydrogen and helium.

Figure 1 shows a schematic view of the compact  $E \parallel B$  analyzer and an illustration of the ion detector plate. The end-loss ions passing through the entrance aperture (2 mm in diameter) are analyzed with parallel magnetic and electric fields. The entrance aperture also serves as an electrode for the accelerator/decelerator on which a few hundred volts is usually applied. Both magnetic and electric fields are perpendicular to the plane of the figure. The shaded area represents the cross section of the pole piece of the  $45^\circ$  deflection magnet for energy analysis. The gap width of the magnet is 12 mm. A couple of electrostatic deflection plates which provide an electric field parallel to the magnetic field are installed at the exit of the deflection magnet. The distance between upper and lower plates is designed to be 3 cm from the orbit calculation. A 60 mm  $\times$  80 mm copper-coated epoxy plate is used as an ion detector array. Two sets of detector arrays are shaped on the plate. Each array consists of ten channels of ion collectors for proton and helium ion, respectively. A Faraday cup is located just behind the magnet in order to calibrate the relative sensitivity of each ion detector channel. A vacuum chamber and an entrance aperture are made of mild steel for magnetic shielding against the leakage field from the mirror coils.

In the above-mentioned analyzing scheme, first-order focusing of analyzing ions is not obtained due to the use of the  $45^\circ$  deflection magnet. Therefore, it is necessary to calculate the precise orbit of the ions deflected magnetically and electrostatically in the analyzer. We calculated the electric and magnetic fields including the fringe field by the finite element method. The orbit of the ion was calculated with the Runge-Kutta-Gill method by using the above results. Figure 1(b) shows the plots of spots where the incident beams hit on the detector plate with energy 0.4–1.5 keV, which are obtained from the orbit calculation in a typical  $E \parallel B$  field

<sup>a)</sup>Present address: Kawasaki Heavy Industries, Ltd., Japan.

<sup>b)</sup>Present address: Mitsubishi Electric Corporation, Japan.

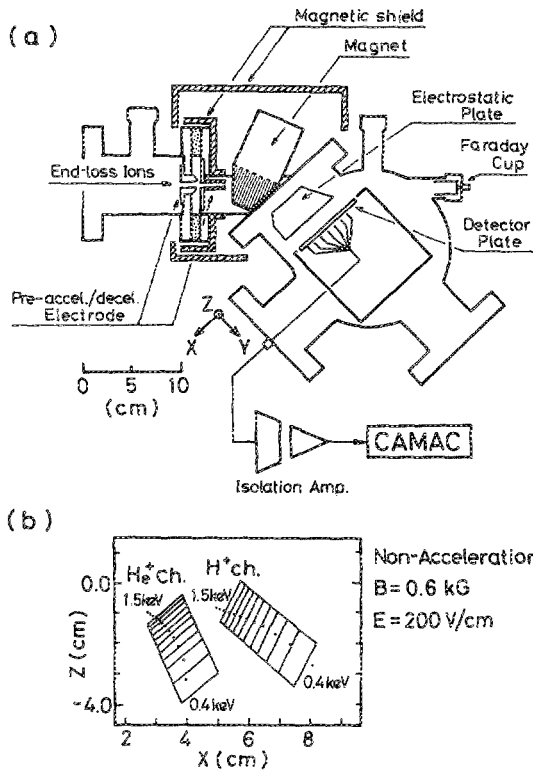


FIG. 1. (a) Schematic view of the compact  $E \parallel B$  type end-loss ion analyzer and (b) illustration of the detector plate designed by using the result of the orbit calculation. Each dot represents the particle hit on the detector plate with energy 0.4–1.5 keV.

( $B = 0.6$  kG,  $E = 200$  V/cm). In this calculation, a pencil beam is assumed to be injected to the entrance aperture and both the accelerator and the decelerator are not used. Strips on the detector plate represent the channels of ion collectors. The layout of the collector channel becomes somewhat complicated compared with that of conventional  $E \parallel B$  analyzers. In the case of analyzers using a  $180^\circ$  bending magnet, the computation of the ion orbit becomes simple by canting the detector plate.<sup>5</sup> In our design, on the other hand, such an advantage cannot be expected. The detector plate is placed parallel to the exit face of the deflection plates in order to simplify the numerical calculation of the orbit.

The energy resolution of each channel was estimated

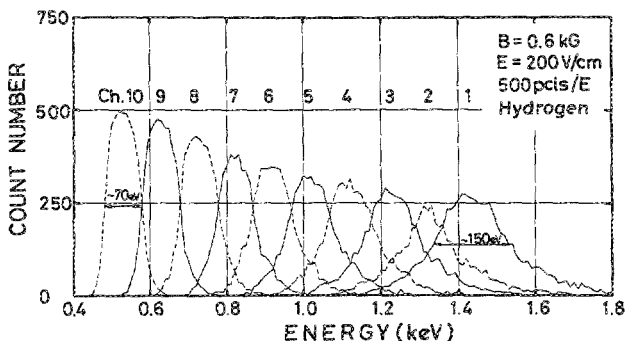


FIG. 2. Result of Monte Carlo simulation of energy resolution in the hydrogen channels (number of particles scored in each channel vs energy). The effects of finite radius and angle of the incident ions and fringe fields in electric and magnetic fields are taken into consideration.

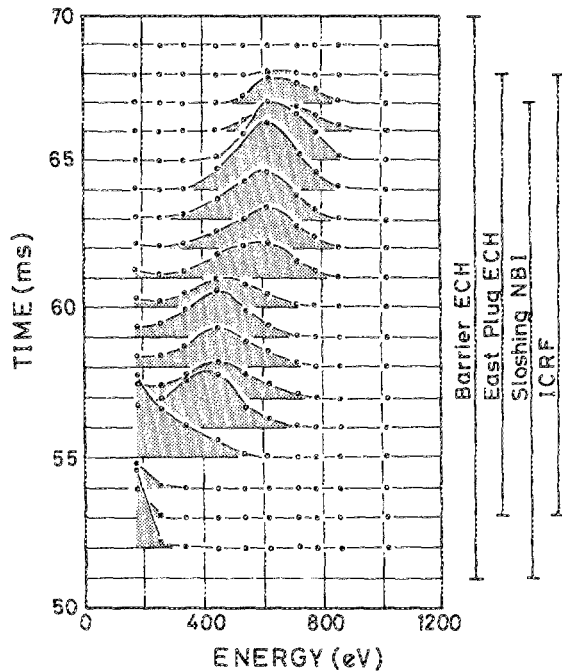


FIG. 3. Sample of the energy spectrum of end-loss ions (ion current vs energy vs time) measured at a weakly plugging mode on GAMMA 10.

with a Monte Carlo simulation in which the effects of the finite radius and angle of the incident ions are taken into consideration. The number of Monte Carlo particles scored in the hydrogen channels is plotted as a function of energy in Fig. 2. FWHM values of 70 and 150 eV are obtained at the lower energy channel (Ch.10) and the higher one (Ch.1), respectively. These values are satisfactory for examining the capabilities of the analyzer.

After calibration experiments with  $H^+$  and  $He^+$  beams, the analyzer was installed at the west end cell of GAMMA 10. The signals of the end-loss ions detected by each channel are transferred to the CAMAC system through the isolation amplifiers. Figure 3 shows a sample of the energy spectrum of end-loss ions as a function of time. After start-up of the heating pulses of neutral beam injection (NBI), electron cyclotron heating (ECH), and ion cyclotron range of frequency (ICRF), the peak value of the energy distribution of end-loss ions was observed to increase indicating the increase of the plasma potential. In this discharge, the plug ECH is applied to the east plug/barrier cell in order to obtain a sufficiently good signal-to-noise ratio.

In summary, a compact  $E \parallel B$  type end-loss ion mass-resolving energy analyzer was designed and fabricated successfully by using a small-angle deflection magnet. The application to the GAMMA 10 tandem mirror showed us that the analyzer has capabilities for the end-loss ion spectrometer. Thus, the compactness of this analyzer will make it possible to measure the spatial profile of end-loss ions in one shot by using several sets of the analyzer.

We would like to acknowledge the members of the GAMMA 10 group for their collaboration. Two of the authors (M. N. and Y. N.) are grateful to Dr. I. Katanuma for helpful discussions about numerical calculations. One of the authors (Y. N.) wishes to thank Professor H. Akimune of

Kyoto University, for his helpful suggestions and encouragement. The numerical calculations were carried out by FACOM VP-200 at the Computer Center of Institute of Plasma Physics in Nagoya University. This work was partially supported by University of Tsukuba project research funds.

<sup>1</sup>A. W. Molvik, *Rev. Sci. Instrum.* **52**, 704 (1981).

<sup>2</sup>J. H. Foote, G. W. Courts, L. R. Pedrotti, L. Schlander, and B. E. Wood, *Rev. Sci. Instrum.* **56**, 1117 (1985).

<sup>3</sup>J. H. Foote, B. E. Wood, M. D. Brown, and G. M. Curnow, *Rev. Sci. Instrum.* **56**, 1786 (1986).

<sup>4</sup>A. L. Roquemore, G. Gammel, G. W. Hammett, R. Kaita, and S. S. Med-

ley, *Rev. Sci. Instrum.* **56**, 1120 (1985).

<sup>5</sup>C. J. Armentrout, G. Bramson, and R. Evanko, *Rev. Sci. Instrum.* **56**, 2101 (1985).

<sup>6</sup>Y. Nakashima, M. Yokoyama, K. Yatsu, and S. Miyoshi (unpublished).

<sup>7</sup>T. Cho, M. Ichimura, M. Inutake, K. Ishii, A. Itakura, I. Katanuma, Y. Kiwamoto, A. Mase, S. Miyoshi, Y. Nakashima, T. Saito, K. Sawada, D. Tsubouchi, N. Yamaguchi, and K. Yatsu, *Proceedings of the Twelfth International Conference on Plasma Physics and Controlled Nuclear Fusion Research, Kyoto, 1986* (International Atomic Energy Agency, Vienna, 1987), Vol. 2, p. 243.

<sup>8</sup>T. Cho, J. H. Foote, Y. Nakashima, K. Ishii, H. Sugawara, M. Yokoyama, T. Segawa, T. Kondoh, I. Katanuma, Y. Kiwamoto, and S. Miyoshi, *J. Phys. Soc. Jpn.* **56**, 3775 (1987).

<sup>9</sup>M. Nemoto, K. Tobita, Y. Kusama, and H. Takeuchi, *J. Jpn. Plasma Sci. Nucl. Fusion Research* **59**, Suppl. 91 (1988) (in Japanese).